Report

Mutations of the *PAX6* Gene Detected in Patients with a Variety of Optic-Nerve Malformations

Noriyuki Azuma,[1,2] Yuki Yamaguchi,[3] Hiroshi Handa,[3] Keiko Tadokoro,[2] Atsuko Asaka,[2] Eriko Kawase,[1,2] and Masao Yamada[2]

[1]Department of Ophthalmology, National Center for Child Health and Development, and [2]Department of Genetics, National Research Institute for Child Health and Development, Tokyo; and [3]Department of Biomolecular Engineering, Frontier Collaborative Research Center, Tokyo Institute of Technology, Yokohama, Japan

The *PAX6* gene is involved in ocular morphogenesis and is expressed in the developing central nervous system and numerous ocular tissues during development. *PAX6* mutations have been detected in various ocular anomalies, including aniridia, Peters anomaly, corneal dystrophy, congenital cataracts, and foveal hypoplasia. However, it has not been identified in patients with optic-nerve malformations. Here, we identified novel mutations in eight pedigrees with optic-nerve malformations, including coloboma, morning glory disc anomaly, optic-nerve hypoplasia/aplasia, and persistent hyperplastic primary vitreous. A functional assay demonstrated that each mutation decreased the transcriptional activation potential of PAX6 through the paired DNA-binding domain. PAX6 and PAX2 are each thought to downregulate the expression of the other. Four of the detected mutations affected PAX6-mediated transcriptional repression of the *PAX2* promoter in a reporter assay. Because *PAX2* gene mutations were detected in papillorenal syndrome, alternation of PAX2 function by *PAX6* mutations may affect phenotypic manifestations of optic-nerve malformations.

Previous ophthalmoscopy and medical imaging studies have established a variety of clinical entities in optic-nerve malformation (Brown and Tasman 1983), since numerous tissues and developmental events contribute to the optic-nerve architecture. The optic nerve first arises as the optic stalk between the forebrain and optic vesicle at 3 wk human gestation. At 5–6 wk, mesenchymes and vessels invade through the embryonic fissure, a transiently appearing ventral cleft of the optic stalk and optic cup, into the vitreous cavity. Nerve fibers of retinal ganglion cells then begin to project into the CNS at 8–10 wk. In the middle stage, the optic nerve is coated with a collagen sheath and propped up by glial cells, and the nerve head is transiently covered with glial cells and hyaloid vessels. In this series of events, developmental failure of the embryonic fissure (resulting in coloboma), ret-

inal ganglion cells (optic-nerve hypoplasia/aplasia), and hyaloid vessels (persistent hyperplastic primary vitreous) cause disease (Brown and Tasman 1983). Most of these anomalies are sporadic, but autosomal dominant inheritance has been reported in families with coloboma of the optic nerve (CON [MIM 120430]) and optic-nerve hypoplasia (ONH [MIM 165550]). Mutations causing autosomal dominant syndrome have been identified in two transcription factor genes. The *PAX2* gene, one of nine known paired box genes, is expressed in the developing optic stalk, the ventral half of the optic cup, and the kidney, and its mutations cause papillorenal syndrome (PRS [MIM 120330]) (Sanyanusin et al. 1995). *HESX1* gene mutations, expressed in the ventral half of the forebrain, Ratke's pouch, and pituitary gland, were identified in patients with septo-optic dysplasia (SOD [MIM 182230]) (Dattani et al. 1998). However, there has not been genetic interpretation of various manifestations of optic-nerve malformations.

The *Pax6/PAX6* gene, first isolated as a candidate gene for human aniridia and expressed in developing CNS and various ocular tissues (Walther and Gruss 1991; Nishina et al. 1999), encodes a transcription factor that is involved in eye morphogenesis (Gehring 1996). Genetic analysis

has detected numerous *PAX6* mutations, not only in patients with aniridia but also with other eye anomalies (summarized in the Human *PAX6* Mutation Database). In situ hybridization and immunohistochemistry indicated *PAX6* expression in the developing optic nerve (Walther and Gruss 1991; Nishina et al. 1999), and the small eye (*Sey^H*) mouse mutant with a deletion of the *Pax6* locus showed coloboma, a defect of the initial invagination in the optic stalk and cup (Glaser et al. 1990). However, there is no evidence of *PAX6* mutations in patients with optic-nerve malformations.

We screened for *PAX6* mutations in genomic DNA from 155 individuals with a variety of congenital optic-nerve malformations by use of PCR-SSCP analysis. PCR primers used to amplify *PAX6* exons were synthesized on the basis of the reported sequence (Glaser et al. 1992); the primer sequences can be found in appendix A (online only), and the conditions of PCR and SSCP analyses were described elsewhere (Azuma et al. 1999). Nucleotide sequences were determined directly or after cloning into plasmid pUC18 by use of a Sequenase version 2 kit (Amersham) with PCR primers or universal primers in pUC18. Eight mutations were detected.

Patient 1, a 5-year-old girl, had bilateral morning glory disc anomaly. Mutation analysis identified 619C→T nucleotide substitution (according to GenBank accession number M93650), which is expected to result in P68S (fig. 1*a*). Patient 2, a 21-year-old male, had bilateral ONH and 1030C→T (Q205X) (fig. 1*b*). Patient 3, a 1-year-old boy, had an iris anomaly, large coloboma of the optic nerve, retina, and choroids, a remnant of hyaloid vessel proliferation (persistent hyperplastic primary vitreous) bilaterally, and growth and mental retardation; mutation analysis identified 1190T→C (F258S) (fig. 1*c*). Patient 4, a 2-year-old boy, had bilateral ONH, growth and mental retardation, an enlarged ventricle by computed tomography (CT) study, multiple spike and wave bursts by electroencephalogram, and vesicoureteral reflux; mutation analysis identified 1292G→T (S292I) (fig. 1*d*). Patient 5, a 1-year-old girl, had Peters anomaly in the left eye and slight corneal opacity, deep excavation of the optic-nerve head in the right eye, and 1504T→C (S363P) (fig. 1*e*). Patient 6, a 2-mo-old girl, had microphthalmos in the right eye, iris dysplasia and optic-nerve aplasia with a remnant of the hyaloid vessels in the left eye, and 1550A→G (Q378R) (fig. 1*f*). Patient 7, a 19-year-old male, had bilateral ONH and 1558A→G (M381V) (fig. 1*g*). Patient 8, a 4-mo-old girl, had bilateral optic-nerve aplasia and 1588A→G (T391A) (fig. 1*h*). Further clinical details can be found in appendix A (online only).

All patients except patients 3 and 4 had normal growth, intelligence, results of physical examination, and appearance on CT. Each had a normal karyotype. The mutations detected here occurred on one of the alleles (were thus heterozygous) and were not detected in unaffected

immediate family members or in >100 normal individuals, indicating sporadic occurrence. Since mutations of the *PAX2* gene were detected in patients with optic-nerve anomalies associated with renal anomaly (PRS) (Sanyanusin et al. 1995), we screened for *PAX2* but failed to detect any mutation in these patients (data not shown).

Although all the mutations are indicated to be sporadic, each occurred in an important amino acid residue, which suggests that they cause disease. Seven of the eight mutations were missense, one of which was positioned in the paired domain (PD), one in the homeodomain (HD), and five in the proline-serine-threonine-rich transactivating domain (PST). The proline residue at 68 in the PD and the phenylalanine residue at 258 in the HD are conserved throughout all Pax family members identified to date. The serine residues at 292 and 363, the glutamine residue at 378, the methionine residue at 381, and the threonine residue at 391 in the PST are conserved throughout all the vertebrate Pax6 homologues identified to date. Amino acid sequences of the PST are conserved in vertebrates but considerably diversified in invertebrates.

We next performed functional assay of the mutations. The mutant forms of *PAX6* cDNAs, generated by PCR-based in vitro mutagenesis, were cloned into plasmids pBluescript and pCAGGS, the latter of which contains a cytomegalovirus enhancer and chicken β-actin promoter (Yamaguchi et al. 1997; Azuma et al. 1999). Wild-type and mutant forms of PAX6 proteins were synthesized by in vitro transcription and translation by use of rabbit reticulocyte lysate in the presence of [^{35}S] methionine. SDS-polyacrylamide gel electrophoresis and fluorography of the reactions revealed that the PAX6 proteins with expected molecular weights were produced at similar efficiency (data not shown). It is, therefore, unlikely that the mutations affect the efficiency of translation or stability of PAX6 protein.

To examine possible functional changes by the detected mutations, we performed a chloramphenicol acetyltransferase (CAT) assay in mouse embryonic carcinoma P19 cells, which are often used for functional analysis of the *PAX6* gene. First, a CAT-reporter construct carrying six copies of P6CON, the consensus binding sequence of the PAX6 PD (Epstein et al. 1994; Yamaguchi et al. 1997), was used. Wild-type PAX6 strongly activated CAT reporter-gene expression, and the transcriptional activation potential of PAX6 was more or less affected by all the mutations reproducibly, with significant impairment by P68S, Q205X, F258S, and S292I (fig. 2*b*). The mutation within the HD (F258S) impaired the PD-mediated transcriptional activation and is consistent with a report of the functional interplay of the PD and the HD (Mishra et al. 2002).

In the optic stalk and ventral forebrain of the zebrafish embryo, *Pax2* and *Pax6* expression is inversely correlated
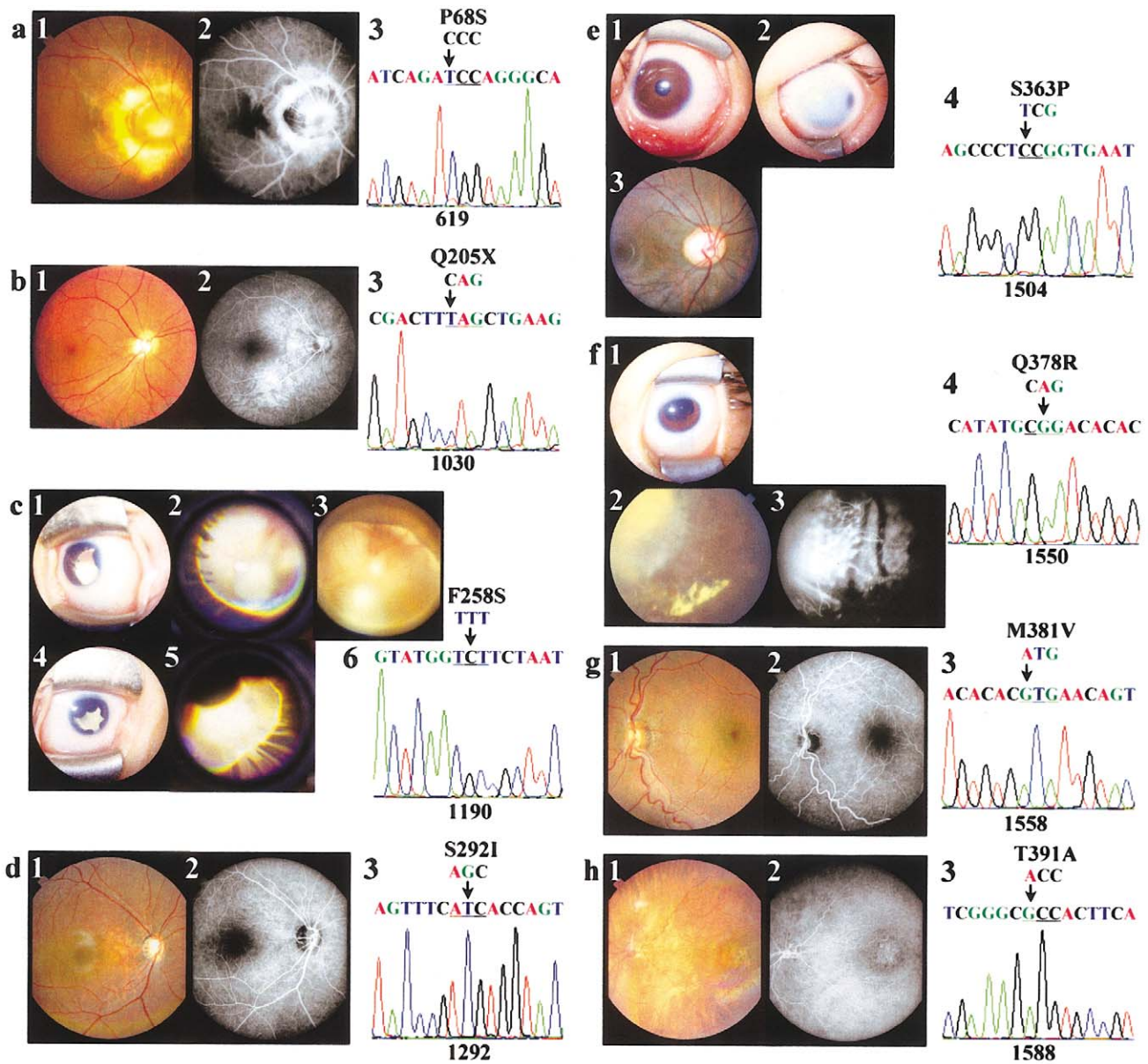
Figure 1 *a,* Fundus photography (*panel 1*) and fluorescein angiography (*panel 2*) of the right eye of patient 1, showing a morning glory disc anomaly. The optic-nerve region is excavated, and white tissue is present at the bottom. *Panel 3,* Mutation analysis identified 619C→T in exon 6 (P68S). *b,* Fundus photography (*panel 1*) and fluorescein angiography (*panel 2*) of the right eye of patient 2, showing a small optic-nerve head surrounded by a hypopigmented ring. *Panel 3,* Mutation detection of 1030C→T in exon 8 (Q205X). *c,* Photographs showing the anterior segments (*panel 1* and *panel 4*) and fundus (*panel 2, panel 3,* and *panel 5*) of patient 3. The iris was dysplastic and the posterior fundus showed large coloboma of the optic nerve, retina, and choroid. Hyaloid vessel proliferation is seen in the vitreous cavity. *Panel 6,* Mutation detection of 1190T→C in exon 10 (F258S). *d,* Fundus photography (*panel 1*) and fluorescein angiography (*panel 2*) of the right eye of patient 4, showing ONH. *Panel 3,* Mutation detection of 1292G→T in exon 10 (S292I). *e,* The right eye of patient 5 has a slight corneal opacity and iridocorneal adhesion (*panel 1*) and deep excavation of the optic-nerve head (*3*). The left eye has substantial corneal opacity (*panel 2*). *Panel 4,* Mutation detection of 1504T→C in exon 12 (S363P). *f,* The anterior segment (*panel 1*), fundus photography (*panel 2*), and fluorescein angiography (*panel 3*) of the left eye, with optic-nerve aplasia, of patient 6. The iris was dysplastic, and the optic-nerve head and retinal vessels were absent, with a remnant of the hyaloid vessels. *Panel 4,* Mutation detection of 1550A→G in exon 12 (Q378R). *g,* Fundus photography (*panel 1*) and fluorescein angiography (*panel 2*) of the left eye, with ONH, of patient 7. *Panel 3,* Mutation analysis identified 1558A→G in exon 12 (M381V). *h,* Fundus photography (*panel 1*) and fluorescein angiography (*2*) of the left eye, with optic-nerve aplasia, of patient 8. *c,* Mutation analysis identified 1588A→G in exon 12 (T391A).
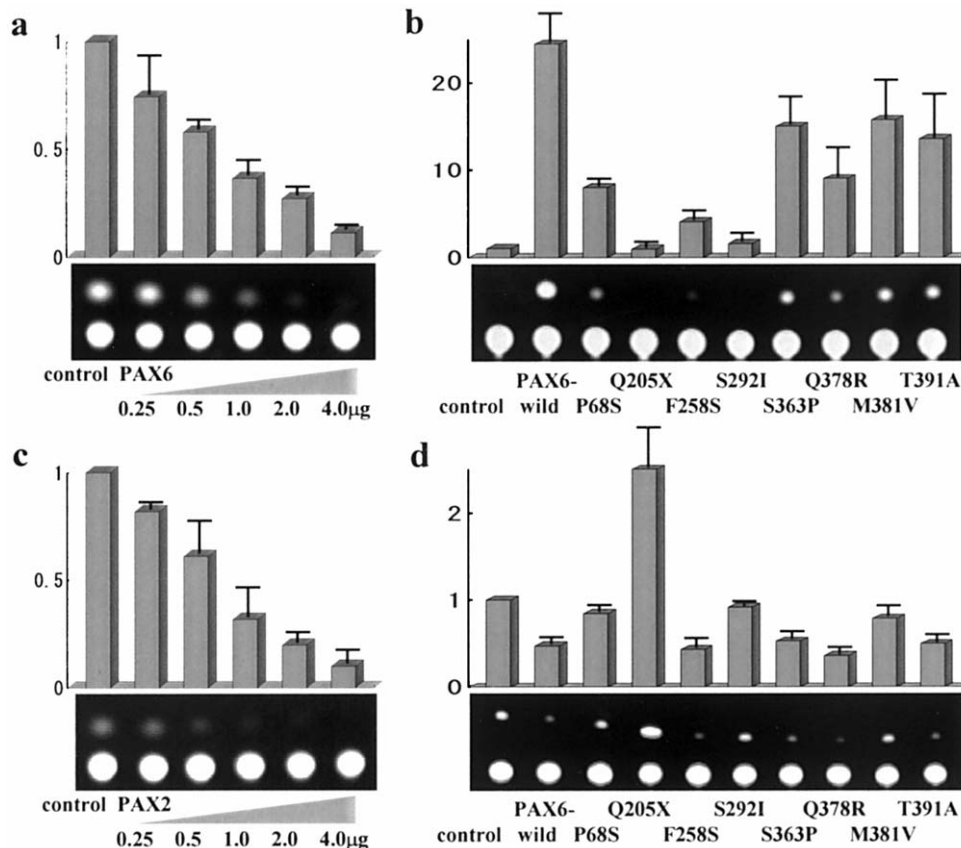
Figure 2   Effects of PAX6 on *PAX2* (*a*) and of PAX2 on *PAX6* (*c*). CAT activities were measured in P19 cells after cotransfection of effecter and reporter constructs. Total volume of DNA was adjusted with an empty vector, pBluescript. Cell extracts were prepared after 48 h and assayed for CAT activities by use of a FAST CAT Green Reagent (Molecular Probes). The CAT activity was quantified by measurement with a phospho-fluor-imager (Molecular Dynamics) and illustrated in a fold-activation, compared with the condition with the vector alone. The levels of *PAX2* were suppressed with increasing amounts of wild type of PAX6, and vice versa. *b*, Transactivating potential of PAX6 mutants. 0.1 μg of effecter construct and 1 μg of reporter constructs were cotransfected in P19 cells. Transcription level from P6CON was disturbed significantly by P68S, Q205X, F258S, and S292I mutants and slightly by S363P, Q378R, M381V, and T391A mutants. *d*, Effects of PAX6 mutants on *PAX2* expression. One μg of effecter construct and 1 μg of reporter constructs were cotransfected in P19 cells. The decreasing level of PAX6 was significantly disturbed with the P68S, Q205X, S292I, and M381V mutants. Each photograph of CAT assay under the bar graph is representative of at least three independent experiments.

under the control of sonic hedgehog signaling (Macdonald et al. 1995). Data indicating reciprocal transcriptional repression of *Pax2* and *Pax6* also were obtained using mouse homologues (Schwarz et al. 2000). Thus, although PAX2 and PAX6 were initially considered to be transcriptional activators, they also may inhibit transcription of some genes to exert their roles during development. We next examined the effect of PAX6 and PAX2 proteins on activities of *PAX2* and *PAX6* gene promoters, respectively. A CAT-reporter construct carrying an ~2-kb *PAX6* promoter region (the 1285th to 3381st nucleotides in GenBank accession number U63833), or a 1.2-kb *PAX2* promoter region (the −1002nd to +190th nucleotides in GenBank accession number U45245) was used. When an increasing amount of the *PAX6* or *PAX2* expression construct was cotrans-

fected into P19 cells with a constant amount of the *PAX2* or *PAX6* reporter construct, each CAT activity decreased in a dose-dependent manner, indicating that PAX6 represses *PAX2* gene expression and vice versa (fig. 2*a* and 2*c*). By use of this assay system, we evaluated possible effects of the PAX6 mutations on *PAX2* promoter activity. Four expression constructs carrying P68S, Q205X, S292I, or M381V mutations failed to repress the *PAX2* promoter activity, unlike the wild-type PAX6 and other mutant constructs (fig. 2*d*). These mutations were found with morning glory disc anomaly or ONH and caused a functional change in our experimental system. Because *PAX2* mutations were also found in coloboma and ONH (Sanyanusin et al. 1995), we speculate that failure of the PAX6-PAX2 regulatory circuit may affect phenotypic manifestations of these anomalies. Ex-

pression of the CAT-reporter gene was probably inhibited by endogenous PAX6 protein to some extent and stimulated by Q205X through its dominant-negative action on endogenous *PAX6,* as suggested elsewhere (Singh et al. 1998). Numerous processes are needed for optic-nerve formation, so *PAX2* and *PAX6* may cooperate in optic-nerve formation or occasionally share tasks; for example, opening and closing the embryonic fissure and mutations of either gene cause similar phenotypic changes.

Our patients had a wide variety of optic-nerve malformations, in which a full series of disease-causing events of optic-nerve malformation—including embryonic fissure (coloboma), retinal ganglion cells (ONH/aplasia), and hyaloid vessels (persistent hyperplastic primary vitreous)—are included (Brown and Tasman 1983). Because *Pax6/PAX6* is expressed in numerous tissues important for optic-nerve development—including the CNS, optic stalk, and retinal progenitors at an early stage, and retinal ganglion cells at a late stage—it is not surprising that many more variable phenotypes are caused by *PAX6* mutations than by *PAX2* mutations.

Genetic analysis indicated that haploinsufficiency of the gene causes the classical aniridia phenotype, in which all eye tissues are affected. Most mutations detected in aniridia result in premature translational termination on one of the alleles (Martha et al. 1994). In contrast, most missense mutations generate distinctive nonaniridia phenotypes—including anterior segment anomalies, congenital cataracts, and foveal hypoplasia—in which certain eye tissue is affected (Hanson et al. 1999). Because most of the amino acid residues are conserved, distinct missense mutations may alter the degree and specificity of DNA binding and transcriptional regulation by PAX6 protein to a different extent (Yamaguchi et al. 1997; Azuma et al. 1999). Some missense mutations are thought to be recurrently associated with a specific phenotype in eye anomalies. Two patients with an R128C mutation, independently identified in Japan and Europe, had the same phenotype, with foveal hypoplasia (Azuma et al. 1996; Hanson et al. 1999). Mutations associated with Peters anomaly were in the N-terminal subdomain of the PD (van Heyningen and Williamson 2002). In contrast, a missense mutation in the alternatively spliced exon was associated with a variety of ocular anomaly phenotypes (Azuma et al. 1999). No distinct positional effect of the missense mutations on phenotypic manifestation of optic-nerve malformations was found in the present study. Because the *Pax6/PAX6* gene is expressed repeatedly throughout ocular tissues, these missense mutations probably disturb PAX6 protein function in different ways, which result in various phenotypes.

Besides eye anomalies, patient 3 was mentally retarded, and patient 4 had an enlarged CNS ventricle and a urinary anomaly. *PAX6* plays an important role in CNS development, and CNS malformation and mental retardation associated with *PAX6* mutations have been reported (Malandrini et al. 2001; Sisodiya et al. 2001). However, gene expression in the urinary tract was not reported. It is unknown if patient 4 carries compound mutations of the separate genes related to eye or urinary-tract development, or whether *PAX6* is slightly, or for a short time, expressed in the urinary tract. Because *PAX2* is expressed in the kidney, extensive analysis of expression and correlation of *PAX6* and *PAX2* throughout development would validate the significance of the genes in pathogenesis of the diseases in which multiple organs are involved.

Acknowledgment

Electronic-Database Information

Accession numbers and URLs for data presented herein are as follows:

GenBank, http://www.ncbi.nlm.nih.gov/Genbank/ (for human *PAX6* mRNA [accession number M93650], human *PAX6,* promoter and exons 1 and 2 [accession number U63833], human *PAX2,* promoter and exon 1 [accession number U45245])

Human *PAX6* Mutation Database, http://pax6.hgu.mrc.ac.uk/Tables/tables.htm

Online Mendelian Inheritance in Man (OMIM), http://www.ncbi.nlm.nih.gov/Omim/ (for CON, ONH, PRS, and SOD)

References

Azuma N, Nishina S, Yanagisawa H, Okuyama T, Yamada M (1996) PAX6 missense mutation in isolated foveal hypoplasia. Nat Genet 13:141–142

Azuma N, Yamaguchi Y, Handa H, Hayakawa M, Kanai A, Yamada M (1999) Missense mutation in the alternative splice region of the PAX6 gene in eye anomalies. Am J Hum Genet 65:656–663

Brown GC, Tasman WS (1983) Congenital anomalies of the optic disc. Grune & Stratton, New York

Dattani MT, Martinez-Barbera JP, Thomas PQ, Brickman JM, Gupta R, Martensson IL, Toresson H, Fox M, Wales JK, Hindmarsh PC, Krauss S, Beddington RS, Robinson IC (1998) Mutations in the homeobox gene *HESX1/Hesx1* associated with sepro-optic dysplasia in human and mouse. Nat Genet 19:125–133

Epstein JA, Cai J, Glaser T, Jepeal L, Maas RL (1994) Identification of a Pax paired domain recognition sequence and

evidence for DNA-dependent conformational changes. J Biol Chem 269:8355–8361

Gehring WJ (1996) The master control gene for morphogenesis and evolution of the eye. Genes Cells 1:11–15

Glaser T, Lane J, Housman D (1990) A mouse model of the aniridia-Wilmus tumor deletion syndrome. Science 250:823–827

Glaser T, Walton DS, Maas RL (1992) Genomic structure, evolutionary conservation and aniridia mutation in the human PAX6 gene. Nat Genet 1:232–239

Hanson I, Churchill A, Love J, Axton R, Moore T, Clarke M, Meire F, van Heyningen V (1999) Missense mutations in the most ancient residues of the PAX6 paired domain underlie a spectrum of human congenital eye malformations. Hum Mol Genet 8:165–172

Macdonald R, Barth KA, Xu Q, Holder N, Mikkola I, Wilson SW (1995) Midline signalling is required for Pax gene regulation and patterning of the eyes. Development 121:3267–3278

Malandrini A, Mari F, Palmeri S, Ganbelli S, Berti G, Bruttini M, Bardelli AM, Williamson K, van Heyningen V, Renieri A (2001) PAX6 mutation in a family with aniridia, congenital ptosis, and mental retardation. Clin Genet 60:151–154

Martha A, Ferrell RE, Mintz-Hittner H, Lyons LA, Saunders GF (1994) Paired box mutations in familial and sporadic aniridia predicts truncated aniridia proteins. Am J Hum Genet 54:801–811

Mishra R, Gorlov IP, Chao LY, Singh S, Saunders GF (2002) PAX6, paired domain influences sequence recognition by the homeodomain. J Biol Chem 277:49488–49494

Nishina S, Kohsaka S, Yamaguchi Y, Handa H, Kawakami A, Fujisawa H, Azuma N (1999) PAX6 expression in the developing human eye. Br J Ophthalmol 83:723–727

Sanyanusin P, Schimmenti LA, McNoe LA, Ward TA, Pierpont ME, Sullivan MJ, Dobyns WB, Eccles MR (1995) Mutation of the PAX2 gene in a family with optic nerve colobomas, renal anomalies and vesicoureteral reflux. Nat Genet 9:358–364

Schwarz M, Cecconi F, Bernier G, Andrejewski N, Kammandel B, Wagner M, Gruss P (2000) Spatial specification of mammalian eye territories by reciprocal transcriptional repression of Pax2 and Pax6. Development 127:4325–4334

Singh S, Tang HK, Lee JY, Saunders GF (1998) Truncation mutations in the transactivation region of PAX6 results in dominant-negative mutants. J Biol Chem 273:21531–21541

Sisodiya SM, Free SL, Williamson KA, Mitchell TN, Willis C, Stevens JM, Kendall BE, Shorvon SD, Hanson IM, Moore AT, van Heyningen V (2001) PAX6 haploinsufficiency causes cerebral malformation and olfactory dysfunction in humans. Nat Genet 28:214–216

van Heyningen V, Williamson KA (2002) PAX6 in sensory development. Hum Mol Genet 11:1161–1167

Walther C, Gruss P (1991) Pax-6, a murine paired box gene, is expressed in the developing CNS. Development 113:1435–1449

Yamaguchi Y, Sawada J, Yamada M, Handa H, Azuma N (1997) Autoregulation of Pax6 transcriptional activation by two distinct DNA-binding subdomains of the paired domain. Genes Cells 2:255–261